Increased Expression of *PDGFA* and *RAF1* in Tumor-Derived Exosomes in Human Colorectal Cancer

Somayeh Vafaei
Iran University of Medical Sciences
marzieh naseri
Iran University of Medical Sciences
margot zoeller
Heidelberg University
leili saeednejad zanjani
Iran University of Medical Sciences
razieh karamnia
Royan Institute for Stem Cell Biology and Technology
yuzhen gao
zhejiang university
hadi ahmadi amoli
Iran University of Medical Sciences
marzieh ebrahimi
Royan Institute for Stem Cell Biology and Technology
Zahra Madjd (zahra.madjd@yahoo.com)
Iran University of Medical Sciences https://orcid.org/0000-0001-7329-2583

Research Article

Keywords: Colorectal cancer, Bioinformatics analysis, Tumor-derived exosomes, PDGFA, RAF1.

Posted Date: November 8th, 2021

DOI: https://doi.org/10.21203/rs.3.rs-1033894/v1

Abstract

Background: Overexpression of tumor markers in Extracellular vesicles (EV), especially in tumor-derived exosomes (TDEs), is implicated in metastasis. However, identifying the specific content of Ev's roles in CRC diagnosis or prognosis requires further validation by bioinformatics and clinical investigations.

Methods: In the current study, we explored molecular markers shared between TDEs and circulating tumor cells (CTCs) in the blood of cancer patients to identify candidate genes involved in CRC metastasis. Common markers were analyzed in gene expression profiles of two studies (GSE31023 and GSE72577).

Results: In blood samples from 20 CRC patients, the expression of candidate genes was assessed by real-time PCR in CTC, TDEs, and microvesicles (MVs), and the expression levels were correlated with clinicopathological features. To further confirm, the expression of candidate genes was investigated in exosomes derived from the parental HT-29 colorectal cancer cell line (HT-29-EXOs), and CSC-enriched spheroids (CSC-EXOs) derived thereof. Gene ontology (GO) analysis suggested platelet-derived growth factor A (*PDGFA*) and proto-oncogene, Serine/Threonine kinase Raf-1 (*RAF1*) as new CRC candidate markers in CTCs and TDEs. According to real-time PCR, expression of *PDGFA* (P=0.0086) and *RAF1* (P=0.048) were upregulated in TDEs but significantly decreased (P=0.0001) in MVs. Furthermore, expression in CSC-EXOs (P=0.0004) was increased compared to HT-29-EXOs.

Conclusion: *PDGFA* and *RAF1* mRNA are higher in CSC-EXOs than in HT-29-EXOs, which correlates with higher expression in CSC than the primary tumor. Notably, as no increase was observed in MVs, *PDGFA* and *RAF1* mRNA appear to be actively recruited into TDE.

Background

Colorectal cancer (CRC) is ranked as third in both incidence and mortality rates among cancers worldwide and the incidence rate is rapidly increasing in developing countries. CRC frequently is diagnosed at the late stages by invasive biopsy techniques (colon/sigmoidoscopy) [1]. This invasive histological examination hampers regular preventive medical surveillance and post-surgery monitoring. Hence, shifting to non-invasive methods especially based on blood-born molecular markers could possibly allow for earlier detection of primary tumors as well as recurrence and metastases [2, 3]. Nucleic acid biomarkers are available in biological fluids, and in several malignancies so-called “liquid biopsies” provided ideal biomarkers for diagnosis and prognosis [4, 5]. Successful tracing of tumors by liquid biopsies relies on the identification of molecular signatures of circulating tumor cells (CTCs) and cancer stem cells (CSCs), in addition to tumor-derived vesicles such as tumor-derived exosomes (TDEs) and microvesicles (MVs) [6].

A considerable number of CTCs and CSCs separate from primary and metastatic tumor cells, which undergo a sequence of epithelial to mesenchymal transition (EMT) steps, provoking invasion, intravasation, circulation, extravasation, pre-metastatic niche preparation, and colonization at secondary sites [7]. Single or clustered CTCs circulating to distant sites or "self-seeding" can prolong tumor cell

survival and their escape from immune cells by multiple mechanisms [8, 9]. CTCs, isolated from the circulation, provided valuable information on tumor biology and cancer cell dissemination [10]. The most common obstacles are heterogeneity and plasticity of CTC as well as their rarity making detection, enumeration and molecular characterization very challenging [11]. CSCs are a subpopulation of CTCs with special characteristics including self-renewal, infinite proliferation and multi-lineage differentiation. CSCs are engaged in carcinogenesis, relapse, and chemoresistance [12, 13].

Exosomes, 30–150 nm nanovesicles and microvesicles (100–350 nm), two major subtypes of extracellular vesicles (EVs), are released into the body's fluids, including the blood [14]. Tumor-derived EV modulates cellular activities in recipient cells by transferring genetic information from cancer cells. Exosomes are endosomal-derived vesicles, which are secreted at the end of the endocytic pathway, when multivesicular bodies fuse with the plasma membrane [15]. Exosomes contain heterogeneous cargoes including lipids, proteins, DNAs, and RNAs (mRNA, miRNA, long non-coding RNA, circular RNA) as well as specific markers like *CD9, CD63, CD81, Alix, flotillin-1* and tumor susceptibility 101 *(TSG101)* [16]. TDEs contribute to immunosuppression, inflammation, angiogenesis, and fibrosis and account for organ-selection of the pre-metastatic niche [17]. Notably, exosomes derive from selected microdomains and are actively loaded with their cargo during invagination of late endosomes into multivesicular bodies. Distinct to exosomes, microvesicles bud off/fission directly from the plasma membrane. They are a heterogeneous population, not displaying unique markers [18].

According to the derivation from defined membrane microdomains and the selective cargo recruitment, TDEs could possibly compensate for gaps in knowledge on CTC activities, due to CTC rarity, fragility, and short life, whereas TDEs are abundant, comparably stable, with good enrichment by easy-to-handle isolation procedures [19, 20]. Nonetheless, the content of TDE has not yet been elaborated in detail.

Based on two studies reporting on common biomarkers in CTCs and EVs (gene expression profile of GSE31023 and GSE72577 from GEO database) and cancer-associated gene searches, we became particularly interested in platelet-derived growth factor A (*PDGFA*) and *RAF1* (Raf-1 proto-oncogene, Serine/Threonine kinase) [20–22].

PDGFA is a proangiogenic factor shown to be essential for tumor metastasis in multiple solid tumor types, including colon [23–25] where high expression was associated with poor survival in the four cohorts of clinical trials [26]. High level of *PDGFA* is also a validated predictor of drug resistance and poor prognosis in CRC patients and plays a crucial role in triggering cancer stemness and maintenance [27]. Platelet-derived *TGF-β* and *PDGF* induce EMT in CTCs and endow migratory and invasive properties allowing to break through the ECM of blood vessels [28].

There are three RAF kinases in human, A-RAF, B-RAF and RAF1 (C-RAF) that are reported to play non-redundant roles. RAF kinases interact with activated RAS, which recruits RAF to the plasma membrane to be activated [29, 30]. Molecular mechanisms underlying expression of KRAS and its effectors and the

subsequent RAS/MAPK pathways await further clarification [31]. Van et al. showed that KRAS can recruit RAF kinase for activation at the membrane from the cytoplasm [32]. Furthermore, RAS-RAF complexation, and RAS-RAF interaction was proven in colorectal cancer [33] but it attracts much more debate in colorectal cancer exosomes. Ras family members have been found in a variety of vesicles [34, 35] and Beckler et al were the first to specifically detect KRAS in exosomes [36].

Proto-oncogene *RAF1* transduces phosphorylation signals from the cell membrane to the nucleus in sequential activation of *MAPK/ERK* pathway (also known as the *Ras-Raf-MEK-ERK* pathway) [34]. Silencing or pharmacological inhibition of *RAF1* impairs clonogenic and tumourigenic capacity of CRC cells and restores apicobasal polarity and formation of tight junctions in cancer cells [36]. *RAS* mutations are negative predictors of response to anti-*EGFR* antibodies. Hyperactivation of the *RAS-RAF* signaling pathway is associated with metastasis, angiogenesis, and poor outcomes of patients in CRC [37]. Where the oncogenic *RAS* activated *MAPK* and *PI3K/AKT* pathways are considered the main effectors in treatment resistance [38, 39].

In the current research, we approached investigating potential common markers between TDEs and CTCs that are implicated in cancer development and metastasis. The mRNA expression levels of predicted target genes were evaluated by quantitative real-time polymerase chain reaction (qRT-PCR) in TDEs and MVs isolated from 20 plasma samples of CRC patients and 10 healthy donors as control. Expression levels of these markers were also examined in exosomes derived from the HT-29 colorectal cancer cell line (HT-29-EXOs) and HT-29 CSC-enriched spheroids (CSC-EXOs). We aimed to shed light on a possible correlation between candidate exosomal mRNAs expression levels and CRC progression and on the EVs-associated mRNA signature. Confirmation of our hypothesis, that TDEs reflect tumor state and aggressiveness, could hold tremendous potential as a minimally invasive screen and may provide hints towards new therapeutic options.

Methods

Data Collection and Bioinformatics Analysis

To obtain candidate genes for CTC and TDE in colorectal cancer, two studies (GSE31023 and GSE72577) were selected (https://www.ncbi.nlm.nih.gov/geo/); the Barbazan et al study contained six cancer and three healthy samples [40] and the Dou et al study encompassed three colorectal cancer cell lines (DLD-1, DKO-1 and DKs-8) and the corresponding TDEs [41]. First, we compared markers expressed in all three TDE and CTC, but not the cell lines. The genes common to TDEs and CTCs were selected.

Characteristic biological features of selected genes were assigned according to gene ontology analysis (GO) [42, 43] to molecular functions, biology processes and cellular components using EnrichR (amp.pharm.mssm.edu/Enrichr/), STRING (https://string-db.org/). DisGeNET RDF v7.0 (ref: https://academic.oup.com/nar/article/48/D1/D845/5611674) was used to search for disease-associated markers, with emphasis on tumor growth. Disease classes were ranked based on the gene-

disease associated (GDA) score and tumor growth-associated markers significantly above the mean score (0.06198) were included in the network analysis, generated using Cytoscape Version 3.7.1 [44] with ClueGO plugin (http://apps.cytoscape.org/apps/cluego) [45] based on gene ontology (GO) (http://geneontology.org/) and pathways, including Kyoto Encyclopedia of Genes and Genomes (KEGG) (https://www.genome.jp/kegg/) [46], Reactome (https://reactome.org/) [47], and WikiPathways (https://www.wikipathways.org/index.php/WikiPathways) [48]. DisGeNET integrates both expert-curated databases with text-mined data, covering information on Mendelian and complex diseases [49]. All analyses were performed in the R programming language to reach common molecular markers betweenCTC and TDE.

Cell Culture and Generation of CSC-Enriched Spheroids

The colorectal adenocarcinoma HT-29 cell line was obtained from Iranian Biological Research Center (IBRC). Colonosphere formation was carried out as described [50]. Briefly, HT-29 cells were grown to 70–90% confluence. After washing with pre-warmed phosphate-buffered saline (PBS), cells were detached by trypsin/ EDTA (Gibco, Germany) and single cells were seeded in poly-HEMA (Sigma, USA)-coated plates (low attachment condition) in DMEM/F12 serum-free medium (Gibco, Germany) supplemented with 10 ng/ml of recombinant basic fibroblast growth factor (bFGF, PeproTech, USA), human recombinant epidermal growth factor (EGF, PeproTech, USA), 2% B27 supplement (Gibco, Germany), 2mM L-glutamine (Gibco, Germany), 1% nonessential amino acid (Gibco, Germany), and 1% penicillin–streptomycin (Gibco, Germany). The culture medium was supplemented with bFGF, EGF, and 2% B27 supplement every third day. After ten days, culture supernatant was collected for exosome isolation.

For HT-29 cells culture, exosome-free FBS was obtained after overnight ultracentrifugation of FBS (Gibco, Germany) at 110,000 g, 4°C (45Ti rotor, Beckman Coulter, Fullerton, California). Cells were cultured in DMEM/high glucose media (Gibco, Germany) supplemented with 10% exosome-free FBS, 1% L-glutamine (Gibco, Germany), 100 U/mL of penicillin, and 100 mg/mL streptomycin (Gibco, Germany), and maintained at 37°C, 5% CO_2 in a humidified incubator. For exosome isolation, the culture supernatant was harvested at ~90% confluence.

Clinical Sample Collection

Peripheral blood samples were collected from 20 CRC patients and 10 healthy controls at Bahman and Firozgar hospitals from 2018-2020 under ethical committee approval. Healthy controls were enrolled from people who underwent a routine health checkup without disease detection. Cell-free plasma was isolated from all blood samples using 2000×*g* for 10min and suspended in Qiazole (Qiagen, Germany). Samples were stored at -80°C. Patient information including gender, age, TNM stage, tumor differentiation was also recorded.

Exosome Isolation by Ultracentrifugation

Exosomes were isolated from culture media of the HT-29 cell line, HT-29-derived spheroids and plasma samples from patients and healthy controls using ultracentrifugation. In brief, culture supernatants and plasma samples were centrifuged at 350× g for 10 min and then at 3000×g for 10 min to remove cell debris. To separate MV from other extracellular vesicles, supernatants were centrifuged at 21000×g for 20 min and the pelleted microvesicles were resuspended in PBS and stored in -80°C. The supernatant was passed twice through ultracentrifugationat 110,000g for 120 min (45Ti rotor, Beckman Coulter). The exosome pellets were resuspended in 1ml PBS or lysis buffer [51].

Scanning Electron Microscopy (SEM)

Isolated exosomes were fixed in 2.5% (w/v) glutaraldehyde for 20 min, washed in PBS and were dehydrated using a gradient of ethanol (60%, 80%, 90% and 100%). The exosomes were dried at room temperature for 10 min on glass. To make surface conductive, a coating of 2-5 nm gold-palladium alloy was applied by sputtering (SPI-Module Sputtering, Argon as gas for plasma) before imaging by SEM (EM3200, KYKY and SEM, Seron Technology, AIS-2100, Korea).

Dynamic Light Scattering (DLS) and Protein Concentration Measurement of Exosomes

To determine the size distribution of isolated exosomes, 50 µl of exosome samples were added to 950 µl PBS and analyzed by dynamic light-scattering measurements (Malvern, UK). Protein quantification was performed by a Bicinchoninic acid assay (BCA) protein assay (Pierce BCA Protein Assay Kit, Thermo Fisher Scientific).

Western Blot Analysis (WB)

Lysed samples (inRIPA Lysis and Extraction buffer) were subjected to 12% sodium dodecyl sulfate (SDS) polyacrylamide gel electrophoresis, transferring the separated proteins to polyvinylidene difluoride (PVDF) membranes (Bio-Rad, Hercules, California). After blocking, blots were incubated overnight with primary antibodies (*CD9* (Santacruz, Germany (Cat No. sc-13118)), *CD81* (Santacruz, Germany (Cat No. SC-166029)), *TSG101* (Gentex, U.S.A. (Cat No. GTX70255)) ;1:500), followed by a two-hour incubation with secondary antibody (goat anti-mouse, Invitrogen, USA). Enhanced chemiluminescence substrate (ECLTM, Thermo Fisher Scientific, USA) was used as detection reagent.

RNA Isolation and qRT-PCR

RNeasy Micro Kit from Qiagene (Qiagen Cat No. /ID: 74004) was used to isolate the total RNA from exosomes. To remove genomic DNA contamination, RNA samples were treated with DNase I and then Nanodrop (ThermoFisher Scientific, USA) was used for RNA quantification and the purity was checked by the A260/A280 ratio. Twenty nanogram of total RNAs were used for reverse transcription (RT) to generate cDNAs using PrimeScript RT Reagent Kit (Takara, Japan). SYBR Green real-time master mix was used for qRT-PCR. The corresponding primers were acquired from SinaClon company (Iran) as follow: *GAPDH*: 5'-AACTTTGGCATTGTGGAAGG-3' F and 5'-CACATTGGGGGTAGGAACAC-3' R. *PDGFA*: 5'-

GCC CAT TCG GAG GAA GAG AA-3' F and 5'- CAG ATC AGG AAG TTG GCG GA -3' R. *RAF1*: 5'- GGT GAT AGT GGA GTC CCA GC -3' F and 5'- GGT GAA GGC GTG AGG TGT AG -3' R. The expression levels of *PDGFA* and *RAF1* mRNAs were normalized by *GAPDH* mRNA levels based on the $2^{-\Delta\Delta Ct}$ approach [52].

Statistical Analysis

SPSS software version 22.0 (IBM Corp, USA) was utilized to analyze the data. GraphPad Prism version 8.0 for Windows (GraphPad Software, La Jolla, CA, USA, www.graphpad.com)was used to determine the differences between tumor and normal blood samples. Pearson's $\chi 2$ and Spearman's correlation tests were used to analyze the significance of associations and correlations between *PDGFA* as well as *RAF1* expression and clinicopathological parameters. Kruskal-Wallis and Mann-Whitney *U* tests were applied for pairwise comparisons between groups. In all parts, quantified data are derived from 20 tumors, 10 healthy and cell line-derived exosomes samples, a *p*-value of <0.05 was considered statistically significant. As noted, in the first step, all quantified data was replicated an average of three times.

Ethical Approval

The research ethics committee of Iran University of Medical Sciences issued (IR.IUMS.REC 1395.9221513203) for this study. All procedures including informed consent before surgery from all participants were in accordance with the abovementioned ethical standards. The Ethics Committee of the Bahman and Firozgar Hospitals approved the use of clinical samples. Besides, the patients/participants provided their written informed consent to participate in this study.

Results

Bioinformatics Approach to Select Appropriate Genes Involved in Metastasis

We started searching for upregulated genes expressed in 3 CRC-CTCs [40] and exosomes derived from these CRC lines (TDEs) [41] There have been 410 genes upregulated in CTC and exosomes of these lines (**Table S1)**, with 56 markers overexpressed in TDEs from all three cell lines (**Figure 1A and Table S2)**. These 56 genes included a considerable number of non-coding RNAs, where particular long non-coding RNA (*lncRNA) TPTE* pseudogene 1 (*TPTEP1*) was significantly downregulated. For the remaining genes, network and enrichment analysis of the corresponding proteins according to clustered genes (kmeans) are shown in **Table S3**. However, only 4 of the genes expressed in TDEs of the 3 lines were recovered in CTCs, an additional 6 were overexpressed in CTCs and at least two TDEs derived from these lines (**Figure 1B and Table S2)**. Network and enrichment analysis of the corresponding ten proteins are shown in **Table1 and Figure 1C** and **1D**. Next, we searched for tumor growth-associated genes in CTCs and the TDEs of the 3 CRC lines (DisGeNET RDF v7.0 database). From all 1046 diseases-related genes, 425 were tumor growth-associated genes (**Table S4)** and 92 displayed an above average GDA (gene-disease associated) score. Network and enrichment analysis of the corresponding proteins uncovered 4 proteins, *PDGFA, UBEH2, TPTE* and *YWHAZ* that were also shared between CTC and tumor line exosomes and, in addition, *RAF1*, which clustered with *TPTE* and *YWHAZ*. In fact, *RAF1*, *PDGFA* and *YWHAZ* had the

most shared tumor growth nodes (**Figure S1**). Based on the connectivity and its central importance in colorectal cancer [53-55], *RAF1* was included in downstream analysis.

Next, we examined by EnrichR reactome, molecular functions, biological processes and KEGG pathway analysis in CRC TDE- and CSC- including oncogenesis-related genes (**Table S3)**.The analysis of cellular component, molecular functions and biological processes of our selected genes were associated with apoptotic, *PI3K-Akt* signaling pathway and cell cycle sequentially, substantiating that we had depicted the most relevant biomarkers particularly for metastasis and stemness in CTCs and EVs. Besides, by using the above-mentioned tools, we generated the significant related go-terms for *RAF1* and *PDGFA* genes shown in **Table S5 and Figure 2**. To confirm this hypothesis, the expression of these two candidate genes, where one should keep in mind the association between *RAF1* with *TPTE* and *YWHAZ*, was assessed and compared in exosomes derived from the serum of 20 CRC patients and 10 healthy donors.

Patients' Characteristics

The study comprised blood samples from twenty patients and ten healthy volunteers. Clinical data from all patients were recorded. The mean age of patients whom TDEs were isolated were 59 years (SD = 12.48, range 29-81) and whom MVs were isolated were 59 years (SD = 13.08, range 31-81). The mean age of healthy volunteers were 60 years (SD = 14.79, range 25-90); 6 (60%) of them were aged ≤60 years and 4 (40%) were aged >60.All of the clinicopathological details were indicated in **Table 2**.

Characterization of Isolated Exosomes

TDEs and MVs were isolated from plasma samples of CRC patients and healthy donors through ultracentrifugation. SEM revealed TDEs and MVs presenting a homogeneous, round morphology (**Figure 3A** and **B**) with a Z-average of 133.7 and 920, and a size range of 88.26 ± 10.76 nm and 644 ± 49 nm, respectively, as determined by dynamic light scattering (**Figure 3C** and **D**). In addition, HT-29-EXOs and CSC-EXOs also displayed round morphology in SEM imaging (**Figure 3E** and **F**) and consisted of homogeneous vesicles with a Z-average of 131.2 and 102.8, and a size range of 91.53 ± 9.65 and 79.53 ± 8.46 for HT-29-EXOs and CSC-EXOs, respectively (**Figure 3G** and **H**). Western blot revealed TSG101, CD81 and CD9 exosomes surface markers expression in all three exosome preparations, whereas in the negative control; calnexin (CANX) was not detected (**Figure 4A and B**).

Increased mRNA Expression levels of *PDGFA* and *RAF1* in CRC Patients' TDEs

The nonparametric Kruskal–Wallis and Mann–Whitney *U* tests were utilized to measure the differences between the median mRNA *PDGFA* and *RAF1* expressionlevels in TDEs from CRC patients compared to the healthy control group. The results showed statistically significant differences of *PDGFA* and *RAF1* between CRC patients and healthy controls (*P=0.0086* and *P=0.048*, respectively) **(Figure 5A** and **B)**. The median mRNA expression level of *PDGFA* and *RAF1* was 5.95 and 1.50, respectively. In addition, the median mRNA expression level of their healthy controls was 0.80 and 0.85, respectively. Moreover, Spearman's correlation analysis revealed that the expression pattern of *PDGFA* and *RAF1* genes was

strongly positively correlated with each other's (Spearman's rho, *P=0.0084*) in TDEs **(Figure 5C)**. The results of the Mann–Whitney *U* test also showed a statistically significant difference in the median level of *RAF1* mRNA expression between patients' ages (*p=0.05*). Pearson's χ2 test also revealed no statistically significant association between the mRNA expression levels of *PDGFA* and *RAF1* in TDEs and clinicopathological characteristics, summarized in **Table 3.**

Decreased mRNA Expression levels of *PDGFA* and *RAF1* in CRC Patients'-Derived MVs

Our findings revealed that *PDGFA* and *RAF1* expression levels were decreased in MVs derived from CRC patients compared to the healthy control group ones(all, *P=0.0001*) **(Figure 6A** and **B)**. The median mRNA expression level of *PDGFA* and *RAF1* in CRC Patient and healthy controls-derived MVs were as follows: 0.22 and 0.10 (tumor), 0.95 and 1.0 (healthy), respectively. As described for exosomes, downregulated expression of *PDGFA* and *RAF1* genes in MVs correlated to each other (Spearman's rho,*P=0.0029*) **(Figure 6C)**. Pearson's χ2 test also exhibited no statistically significant association between mRNA expression levels of *PDGFA* and *RAF1* in MVs and clinicopathological parameters that are summarized in **Table 4.** The results of Real-Time PCR did not reveal any statistically significant differences in the median level of *PDGFA and RAF1* mRNA expression with TNM stage and tumor differentiation in TDE (**Figure 7A- D)** and MVs(**Figure 7E-H)**. The results show that there was no statistically significant association between our groups.

High *PDGFA* and *RAF1*Expression in CSC-EXOsCompared to Parental HT-29-EXOs

To further evaluate *PDGFA* and *RAF1* expression levels in exosomes from CSC or differentiated tumor cells phenotypes, CSC-derived[56] exosomes (CSC-EXOs) from CSC-enriched spheroids were compared to those derived from the parental cell line (HT-29-EXOs). RT-PCR analysis revealed upregulated expression of both molecules in CSC-EXOs compared to HT-29-EXOs (*P=0.0004*) (**Figure 8A** and **B)**.

Discussion

CRC metastases arise from disseminated cancer cells; their settlement being suggested to be dictated by TDEs [57, 58]. In view of the inefficacy of current therapeutic protocols in metastasis prevention, detection and functional characterization of metastasis-specific biomarkers are urgently warranted [59].

EMT and stemness have been extensively investigated in CTC [60], where subsets enriched in CSC were of particular interest [61], as an improved understanding of the EMT/CTC/CSC connections may uncover yet unknown pathways of tumor progression and possibly provide hints towards novel therapeutic targets [62].

Besides CTC/CSC, TDEs contribute to EMT, angiogenesis and tumor progression. In addition, TDEs carry selected mRNAs that are shuttled in the CRC microenvironment [63], potentiating cancer progression and affecting CRC patient's prognosis [64, 65]. TDEs also suppress immune responses, promote immune evasion and increase drug/ chemotherapy resistance [66, 67]. The steadily increasing interest in CTC and

TDE biomarkers in relation to tumor metastasis is forced by high-throughput analyses, which allow for simultaneous identification and quantification of multiple mRNAs. Novel bioinformatic tools facilitate integration of this multitude of genes into functional networks [68].

We used bioinformatic tools to search for molecular markers shared between CTCs and TDEs in CRC. For EVs isolation we choose ultracentrifugation, considered the gold standard for exosome isolation [69]. Expression levels of markers, including *PDGFA* and *RAF1*, shared by either CTC and TDE or serum-derived TDEs and MVs were evaluated by RT-PCR. To further validate the engagement of TDE-derived *PDGFA* and *RAF1* in the CSC phenotype and characteristics, their expressions were investigated in HT-29-EXOs compared to CSC-EXOs.

Our results indicate increased expression of both *PDGFA* and *RAF1* in TDEs of CRC patients compared to healthy controls. Unexpectedly, expression of both *PDGFA* and *RAF1* was decreased in MVs from CRC patients compared to healthy controls. Notably, *PDGFA* and *RAF1* expressions were correlated in both TDEs and MVs. Low recovery of *PDGFA* and *RAF1* in MVs is in line with MVs originating from budding membrane domains. However, this does not explain lower recovery than in healthy donors' MV. One possible mechanism could be regulation by non-coding RNA, which requires further exploration as we excluded noncoding RNAs from our analysis. Instead, molecular packaging named selective cargo may well contribute to higher *PDGFA* and *RAF1* recovery in TDEs, where besides active recruitment, silencing of counter regulatory elements can presently not be excluded. Finally, *PDGFA* and *RAF1* mRNA is higher in CSC-EXOs than in HT-29-EXOs indicating their potential correlation with the CSC phenotype.

Thus, with all caution, we assume a possible correlation between increased *RAF1* and *PDGFA* expression in exosomes with tumor progression. This study is the first report touching the increased expression of *RAF1* and *PDGFA* in exosomes derived from CRC patients and CSC-EXOs compared to healthy donor and HT-29 parental-derived exosomes (HT-29-EXOs). Since exosomes content reflects the condition of cells of origin and can lead to modulation in recipient cells by transferring their cargo, as well as based on accumulating evidence of the role of increased expression of *RAF1* and *PDGFA* in tumor progression (invasion, angiogenesis and EMT), we assume some possible correlation between increased *RAF1* and *PDGFA* expression in exosomes with tumor progression.

Accumulating evidence supports that *PDGFA* is an important mediator of EMT that contributes to cancer invasion and angiogenesis. Overexpression of *PDGF-D* showed EMT promotion in prostate cancer cells [70]. The crosstalk between *PDGF* and EMT-related signaling pathways, such as the nuclear factor κ-light-chain-enhancer of activated B cells (*NF-κB*) and chemokine (C-X-C motif) receptor 4 (*CXCR4*), further strengthens *PDGF* playing an important role in EMT. Interestingly, in a study on hepatocellular carcinoma (HCC), *PDGF* was hypothesized to be involved in TGF-β-induced EMT of metastasizing cancer cells [71]. Additional studies on the *TGF-β* enhanced expression of *PDGF* and *PDGFR* via activation of β-catenin and the signal transducer and activator of transcription 3 (*STAT3*) [72]. However, it should be mentioned that unsupervised use of anti-*PDGF* could potentially promote tumor invasion and metastasis, stressing dose-dependence of the molecular mechanism [73]. A study on rectal cancer indicated that mRNA expression of

PDGFA was decreased following anti-*PDGF* treatment and pointed towards *PDGFA* expression being also associated with drug resistance [74]. Moreover, in line with our study, expression was up-regulated under hypoxia as well as in the CSCs and high *PDGFA* expression was associated with poor overall survival [75, 76]. Signaling mostly proceeded through the *EGF–STAT3* pathway with increased levels of *LGR5*, and participation of the *Wnt* signaling pathway in *EGFR*-positive CRCs. Also, in line to our study, RT-PCR confirmed increased *PDGFA* levels in both HCT-116-CSCs and HT-29-CSCs [27]. Our study extends those findings towards the important recovery in TDEs and even more pronounced in CSC-EXOs, which allows for the transfer into target cells.

RAF1 play a carcinogenic role especially in angiogenesis process [38]. Moreover, targeting of *RAF1* by miR-7-5p inhibits endothelial cell proliferation. Inhibition of *RAF1* kinase activity impairs CRC growth. Furthermore, down-regulation of miR-431-5p as well as up-regulation of *FBXL19-AS1* increases *RAF1* expression. Thus, *FBXL19-AS1* knockdown-mediated inhibition of lung cancer progression and the expression of angiogenesis associated proteins could be rescued by *RAF1* overexpression [77, 78].

In summary, in line with these studies, we observed overexpression of *PDGFA* and *RAF1* in exosomes from CRC patients, where overexpressions were associated with poor clinicopathological features. These findings suggest a possible role of TDEs with prometastatic factors, including specific mRNAs, as messengers for primary tumor growth and microenvironment preparation for metastasis.

Additional advantages of mRNA biomarkers deserve discussion. In comparison to DNA, mRNAs provide a solid base for signaling network connectivities. Uncovering signaling networks makes RNAs most important in unraveling protein-RNA complexes and allows identifying potential candidates for follow-up work at the protein level including functional studies. Furthermore, due to translational modulation and post-translational modification, protein levels do not necessarily reflect gene expression levels, a problem that can be circumvented by elaborating RNA levels [79, 80]. Several publications also support the importance of mRNA in CRC. Furthermore, additional publications support the view that both mRNA and protein analysis can confirm each other [81-83]. Finally, again in CRC, liquid biopsy-based mRNA evaluation was suggested providing new insights into potential mRNA indicators that may allow avoiding invasive diagnostic operations.

In spite of that, current study had a few limitations, Firstly, our patients' sample size was small requiring future validation in large cohorts of patients' serum-derived TDEs and CSC-EXOs. Secondly, our findings need confirmation at the protein level. This accounts for clinical serum samples as well as for cell culture-derived exosomes and for *in vivo* controls in mouse models. Though our exosome sample sizes, particularly in the clinical cohort, were too small for a comprehensive protein analysis, this will be possible by the restriction to *PDGFA* and *RAF1*. Thirdly, the mode of functional activity of *PDGFA* and *RAF1* in CRC requires further elaboration including the clarification of preferential actions at the mRNA or the protein level.

This is important as to our knowledge we were the first describing high *PDGFA* and *RAF1* mRNA expression in TDEs from CRC patients and exosomes derived from CSC-enriched spheroids, exosomes being a prerequisite for transfer into host cells, may play potential roles in tumor growth and progression. Additionally, serum-derived TDEs would present an easily accessible, non-invasive tool for early diagnosis, prognosis and therapy control.

Conclusion

Based on our results, *PDGFA* and *RAF1* mRNA are higher in CSC-EXOs than in HT-29-EXOs which correlates with higher expression in CSC than the primary tumor. Notably, as no increase was observed in MVs, *PDGFA* and *RAF1* mRNA appear being actively recruited into TDE. In view of the suggested importance of *PDGFA* and *RAF1* expression in CRC prognosis, further validation has high priority in future plan.

Future perspective: large-scale sample analyses are required to unequivocally sustain the superior validity of mRNA enrichment in CRC TDEs. Moreover, next generation sequencing should focus on blood sample-derived CTCs and TDEs of CTC to unravel a comprehensive signature of metastasizing CRC. Completion of these studies may prove serum-derived TDEs as a highly reliable tool for CRC prognostication and patient management.

Abbreviations

BCA: Bicinchoninic acid assay

bFGF: basic fibroblast growth factor

CAPZA2: Capping Actin Protein of Muscle Z-Line Subunit Alpha 2

CRC: colorectal cancer

CSC-EXOs: HT-29 CSC exosomes

CSCs: cancer stem cells

CTCs: circulating tumor cells

CXCR4: chemokine (C-X-C motif) receptor 4

DLS: dynamic light scattering

EGF: human recombinant epidermal growth factor

EGF–STAT3: Epidermal growth factor signal transducer and activator of transcription 3

EMT: epithelial to mesenchymal transition

EVs: Extra cellular vesicles

GO: Gene ontology

GSEA: Gene set enrichment analysis

HCC: hepatocellular carcinoma

HT-29-EXOs: HT-29 colorectal cancer cell line exosomes

IBRC: Iranian Biological Research Center

LDLRAP1: Low Density Lipoprotein Receptor Adaptor Protein 1

LGR5: Leucine-rich repeat-containing G-protein coupled receptor 5

MAPK/ERK: Ras-Raf-MEK-ERK pathway

MVs: Microvesicles

NF-κB: nuclear factor κ-light-chain-enhancer of activated B cells

NPTN: Neuroplastin

PBS: phosphate-buffered saline

PDGFA: Platelet Derived Growth Factor Subunit A

PPP3R1: Protein Phosphatase 3 Regulatory Subunit B, Alpha

PVDF: polyvinylidene difluoride

RAF1: Raf-1 Proto-Oncogene, Serine/Threonine Kinase

RNF11: Ring Finger Protein

SDS: sodium dodecyl sulfate

SEM: scanning electron microscopy

TDEs: tumor-derived exosomes

TPTE: Transmembrane Phosphatase with Tensin Homology

TSG101: Tumor Susceptibility 101

UBE2H: Ubiquitin Conjugating Enzyme E2

WB: western blot

Wnt: Wnt Family Member 1

YWHAH: Tyrosine 3-Monooxygenase/Tryptophan 5-Monooxygenase Activation Protein Eta

YWHAZ: Tyrosine 3-Monooxygenase/Tryptophan 5-Monooxygenase Activation Protein Zeta

Declarations

Ethics approval and consent to participate

The Research Ethics Committee of Iran University of Medical Sciences issued IR.IUMS.REC 1395.9221513203 for this study. All procedures, including obtaining informed consent from each human participant before surgery, were in accordance with the above-mentioned ethical standards.

Consent for publication

The signed consent ensured that the publisher has theparticipate and author's permission to publish the relevant Contribution. Besides, all of the included studies data were used by reference citation and all of the authors consent to publication.

Availability of Data and Materials

Data sharing is not applicable to this article as no new data were created or analyzed in this study. Analyzed data are openly available in [repository name at http://doi.org/[doi] and reference number.

Competing Interests

The authors whose names are listed certify that they have NO affiliations in any organization or entity with any financial interest and non-financial interest in the subject matter or materials discussed in this manuscript.

Funding

This study is part of a PhD thesis in Department of Molecular Medicine and mainly was funded by Iran University of Medical Sciences (number: 96-01-87-30129).

Author's Contributions

ZM, ME and SV, conceived the presented idea. SV collected the blood samples, run the experimental laboratory tests, analyzed and interpreted data and wrote the first draft. ZM and ME developed, revised and approved the theory. MN performed cell culture and spheroid formation assay. SV performed critical

revisions of the first draft and verified the concept. YG and RK helped in bioinformatics data analysis. HA, colorectal surgery specialists who provided patients' tumor sample and their data. All authors read, approved and discussed the results and contributed to the final manuscript.

Acknowledgements

We are grateful our colleagues in Oncopathology Research Center, Iran University of Medical Sciences for their help and also we would like to thank Dr. Faezeh Shekari for her expertise and assistance in this study.

This project has been conducted by a grant from Cancer Research Center of Cancer Institute of Iran (Sohrabi cancer charity, Grant No: 37353-202-01-97) and also by a grant from Royan Stem Cell Technology Company (RSCT96030202).

References

1. Bray F, Ferlay J, Soerjomataram I, et al. Global cancer statistics 2018: GLOBOCAN estimates of incidence and mortality worldwide for 36 cancers in 185 countries. *CA Cancer J Clin* 2018; 68: 394–424.
   2018/09/13
   . DOI: 10.3322/caac.21492.
2. Punt CJ, Koopman M and Vermeulen L. From tumour heterogeneity to advances in precision treatment of colorectal cancer. *Nat Rev Clin Oncol* 2017; 14: 235-246. 2016
   /12/07
   . DOI: 10.1038/nrclinonc.2016.171.
3. Zhai Z, Yu X, Yang B, et al. Colorectal cancer heterogeneity and targeted therapy: Clinical implications, challenges and solutions for treatment resistance. *Semin Cell Dev Biol* 2017; 64: 107-115. 2016
   /09/01
   . DOI: 10.1016/j.semcdb.2016.08.033.
4. Hench IB, Hench J and Tolnay M. Liquid Biopsy in Clinical Management of Breast, Lung, and Colorectal Cancer. *Front Med (Lausanne)* 2018; 5: 9.
   2018/02/15
   . DOI: 10.3389/fmed.2018.00009.
5. Lopez A, Harada K, Mizrak Kaya D, et al. Liquid biopsies in gastrointestinal malignancies: when is the big day? *Expert Rev Anticancer Ther* 2018; 18: 19–38.
   2017/12/06
   . DOI: 10.1080/14737140.2018.1403320.
6. Vafaei S, Fattahi F, Ebrahimi M, et al. Common molecular markers between circulating tumor cells and blood exosomes in colorectal cancer: a systematic and analytical review. *Cancer Manag Res*

2019; 11: 8669–8698. DOI: 10.2147/CMAR.S219699.

7. Katt ME, Wong AD and Searson PC. Dissemination from a Solid Tumor: Examining the Multiple Parallel Pathways. *Trends Cancer* 2018; 4: 20–37. 2018/02/08. DOI: 10.1016/j.trecan.2017.12.002.
8. Giuliano M, Shaikh A, Lo HC, et al. Perspective on Circulating Tumor Cell Clusters: Why It Takes a Village to Metastasize. *Cancer Res* 2018; 78: 845–852.
2018/02/14
. DOI: 10.1158/0008-5472.Can-17-2748.
9. Kim MY, Oskarsson T, Acharyya S, et al. Tumor self-seeding by circulating cancer cells. *Cell* 2009; 139: 1315-1326. 2010/01/13. DOI: 10.1016/j.cell.2009.11.025.
10. Kang Y and Pantel K. Tumor cell dissemination: emerging biological insights from animal models and cancer patients. *Cancer Cell* 2013; 23: 573–581. 2013/05/18. DOI: 10.1016/j.ccr.2013.04.017.
11. Lei X, Jonathan S and Yong-Jie L. Circulating Tumor Cells: A Window to Understand Cancer Metastasis, Monitor and Fight Against Cancers. *Journal of Cancer Research Updates* 2015; 4: 13–29. DOI: 10.6000/1929-2279.2015.04.01.2.
12. Zhou Y, Xia L, Wang H, et al. Cancer stem cells in progression of colorectal cancer. *Oncotarget* 2018; 9: 33403-33415. 2018
/10/04
. DOI: 10.18632/oncotarget.23607.
13. Fedyanin M, Anna P, Elizaveta P, et al. Role of Stem Cells in Colorectal Cancer Progression and Prognostic and Predictive Characteristics of Stem Cell Markers in Colorectal Cancer. *Curr Stem Cell Res Ther* 2017; 12: 19–30.
2016/09/07
. DOI: 10.2174/1574888x11666160905092938.
14. Li P, Kaslan M, Lee SH, et al. Progress in Exosome Isolation Techniques. *Theranostics* 2017; 7: 789–804.
2017/03/04
. DOI: 10.7150/thno.18133.
15. Lee Y, El Andaloussi S and Wood MJ. Exosomes and microvesicles: extracellular vesicles for genetic information transfer and gene therapy. *Hum Mol Genet* 2012; 21: R125-134. 2012
/08/09
. DOI: 10.1093/hmg/dds317.
16. Kowal J, Arras G, Colombo M, et al. Proteomic comparison defines novel markers to characterize heterogeneous populations of extracellular vesicle subtypes. *Proc Natl Acad Sci U S A* 2016; 113: E968-977. 2016
/02/10
. DOI: 10.1073/pnas.1521230113.
17. Fu Q, Zhang Q, Lou Y, et al. Correction: Primary tumor-derived exosomes facilitate metastasis by regulating adhesion of circulating tumor cells via SMAD3 in liver cancer. *Oncogene* 2019; 38: 5740–

5741.
2019/05/10
. DOI: 10.1038/s41388-019-0830-6.

18. Pan BT and Johnstone RM. Fate of the transferrin receptor during maturation of sheep reticulocytes in vitro: selective externalization of the receptor. *Cell* 1983; 33: 967–978.
1983/07/01
. DOI: 10.1016/0092-8674(83)90040-5.
19. Gold B, Cankovic M, Furtado LV, et al. Do circulating tumor cells, exosomes, and circulating tumor nucleic acids have clinical utility? A report of the association for molecular pathology. *J Mol Diagn* 2015; 17: 209–224. DOI: 10.1016/j.jmoldx.2015.02.001.
20. Shao H, Chung J and Issadore D. Diagnostic technologies for circulating tumour cells and exosomes. *Biosci Rep* 2015; 36: e00292-e00292. DOI: 10.1042/BSR20150180.
21. Fransén K, Klintenäs M, Osterström A, et al. Mutation analysis of the BRAF, ARAF and RAF-1 genes in human colorectal adenocarcinomas. *Carcinogenesis* 2004; 25: 527-533. 2003
/12/23
. DOI: 10.1093/carcin/bgh049.
22. Nie F, Cao J, Tong J, et al. Role of Raf-kinase inhibitor protein in colorectal cancer and its regulation by hydroxycamptothecine. *J Biomed Sci* 2015; 22: 56.
2015/07/17
. DOI: 10.1186/s12929-015-0162-y.
23. Heldin C-H. Targeting the PDGF signaling pathway in tumor treatment. *Cell Commun Signal* 2013; 11: 97–97. DOI: 10.1186/1478-811X-11-97.
24. Paulsson J, Ehnman M and Östman A. PDGF receptors in tumor biology: prognostic and predictive potential. *Future Oncol* 2014; 10: 1695–1708.
2014/08/26
. DOI: 10.2217/fon.14.83.
25. Xu R, Ji J, Zhang X, et al. PDGFA/PDGFRalpha-regulated GOLM1 promotes human glioma progression through activation of AKT. *J Exp Clin Cancer Res* 2017; 36: 193.
2017/12/29
. DOI: 10.1186/s13046-017-0665-3.
26. Halberg N, Sengelaub CA, Navrazhina K, et al. PITPNC1 Recruits RAB1B to the Golgi Network to Drive Malignant Secretion. *Cancer Cell* 2016; 29: 339–353.
2016/03/16
. DOI: 10.1016/j.ccell.2016.02.013.
27. Cheng CC, Liao PN, Ho AS, et al. STAT3 exacerbates survival of cancer stem-like tumorspheres in EGFR-positive colorectal cancers: RNAseq analysis and therapeutic screening. *J Biomed Sci* 2018; 25: 60.
2018/08/03

. DOI: 10.1186/s12929-018-0456-y.

28. Linnekamp JF, Wang X, Medema JP, et al. Colorectal cancer heterogeneity and targeted therapy: a case for molecular disease subtypes. *Cancer Res* 2015; 75: 245–249. 2015/01/17 . DOI: 10.1158/0008-5472.CAN-14-2240.
29. Mason CS, Springer CJ, Cooper RG, et al. Serine and tyrosine phosphorylations cooperate in Raf-1, but not B-Raf activation. *EMBO J* 1999; 18: 2137-2148. 1999 /04/16 . DOI: 10.1093/emboj/18.8.2137.
30. Josse R, Zhang YW, Giroux V, et al. Activation of RAF1 (c-RAF) by the Marine Alkaloid Lasonolide A Induces Rapid Premature Chromosome Condensation. *Mar Drugs* 2015; 13: 3625–3639. 2015/06/10 . DOI: 10.3390/md13063625.
31. Assi M, Achouri Y, Loriot A, et al. Dynamic Regulation of Expression of KRAS and Its Effectors Determines the Ability to Initiate Tumorigenesis in Pancreatic Acinar Cells. *Cancer Res* 2021; 81: 2679–2689. 2021/02/20 . DOI: 10.1158/0008-5472.CAN-20-2976.
32. Van QN, Lopez CA, Tonelli M, et al. Uncovering a membrane-distal conformation of KRAS available to recruit RAF to the plasma membrane. *Proc Natl Acad Sci U S A* 2020; 117: 24258–24268. 2020/09/12 . DOI: 10.1073/pnas.2006504117.
33. Tran TH, Chan AH, Young LC, et al. KRAS interaction with RAF1 RAS-binding domain and cysteine-rich domain provides insights into RAS-mediated RAF activation. *Nature Communications* 2021; 12: 1176. DOI: 10.1038/s41467-021-21422-x.
34. McKay J, Wang X, Ding J, et al. H-ras resides on clathrin-independent ARF6 vesicles that harbor little RAF-1, but not on clathrin-dependent endosomes. *Biochimica et Biophysica Acta (BBA) - Molecular Cell Research* 2011; 1813: 298–307. DOI: https://doi.org/10.1016/j.bbamcr.2010.11.019.
35. Eng SK, Imtiaz IR, Goh BH, et al. Does KRAS Play a Role in the Regulation of Colon Cancer Cells-Derived Exosomes? *Biology (Basel)* 2021; 10 2021/01/21. DOI: 10.3390/biology10010058.
36. Demory Beckler M, Higginbotham JN, Franklin JL, et al. Proteomic analysis of exosomes from mutant KRAS colon cancer cells identifies intercellular transfer of mutant KRAS. *Mol Cell Proteomics* 2013; 12: 343-355. 2012 /11/20 . DOI: 10.1074/mcp.M112.022806.
37. Liu Z, Liu Y, Li L, et al. MiR-7-5p is frequently downregulated in glioblastoma microvasculature and inhibits vascular endothelial cell proliferation by targeting RAF1. *Tumour Biol* 2014; 35: 10177–10184.

2014/07/17
. DOI: 10.1007/s13277-014-2318-x.

38. Borovski T, Vellinga TT, Laoukili J, et al. Inhibition of RAF1 kinase activity restores apicobasal polarity and impairs tumour growth in human colorectal cancer. *Gut* 2017; 66: 1106-1115. 2016 /09/28
. DOI: 10.1136/gutjnl-2016-311547.
39. Kasper S, Reis H, Ziegler S, et al. Molecular dissection of effector mechanisms of RAS-mediated resistance to anti-EGFR antibody therapy. *Oncotarget* 2017; 8: 45898–45917. 2017/05/17
. DOI: 10.18632/oncotarget.17438.
40. Barbazan J, Alonso-Alconada L, Muinelo-Romay L, et al. Molecular characterization of circulating tumor cells in human metastatic colorectal cancer. *PLoS One* 2012; 7: e40476. 2012/07/20
. DOI: 10.1371/journal.pone.0040476.
41. Dou Y, Cha DJ, Franklin JL, et al. Circular RNAs are down-regulated in KRAS mutant colon cancer cells and can be transferred to exosomes. *Sci Rep* 2016; 6: 37982. 2016/11/29
. DOI: 10.1038/srep37982.
42. Mi H, Muruganujan A, Ebert D, et al. PANTHER version 14: more genomes, a new PANTHER GO-slim and improvements in enrichment analysis tools. *Nucleic Acids Res* 2019; 47: D419-D426. 2018/11/09
. DOI: 10.1093/nar/gky1038.
43. Harris MA, Clark J, Ireland A, et al. The Gene Ontology (GO) database and informatics resource. *Nucleic Acids Res* 2004; 32: D258-261. 2003 /12/19
. DOI: 10.1093/nar/gkh036.
44. Shannon P, Markiel A, Ozier O, et al. Cytoscape: a software environment for integrated models of biomolecular interaction networks. *Genome Res* 2003; 13: 2498-2504. 2003 /11/05
. DOI: 10.1101/gr.1239303.
45. Bindea G, Mlecnik B, Hackl H, et al. ClueGO: a Cytoscape plug-in to decipher functionally grouped gene ontology and pathway annotation networks. *Bioinformatics* 2009; 25: 1091-1093. 2009 /02/25
. DOI: 10.1093/bioinformatics/btp101.
46. Kanehisa M, Furumichi M, Sato Y, et al. KEGG: integrating viruses and cellular organisms. *Nucleic Acids Res* 2021; 49: D545-d551. 2020/10/31
. DOI: 10.1093/nar/gkaa970.

47. Wu G and Haw R. Functional Interaction Network Construction and Analysis for Disease Discovery. *Methods Mol Biol* 2017; 1558: 235-253. 2017/02/06. DOI: 10.1007/978-1-4939-6783-4_11.

48. Martens M, Ammar A, Riutta A, et al. WikiPathways: connecting communities. *Nucleic Acids Res* 2021; 49: D613-D621. 2020/11/20. DOI: 10.1093/nar/gkaa1024.

49. Pinero J, Bravo A, Queralt-Rosinach N, et al. DisGeNET: a comprehensive platform integrating information on human disease-associated genes and variants. *Nucleic Acids Res* 2017; 45: D833-D839.
2016/12/08
. DOI: 10.1093/nar/gkw943.

50. Eini L, Naseri M, Karimi-Busheri F, et al. Primary colonospheres maintain stem cell-like key features after cryopreservation. *J Cell Physiol* 2020; 235: 2452-2463. 2019
/10/04
. DOI: 10.1002/jcp.29150.

51. Taghikhani A, Hassan ZM, Ebrahimi M, et al. microRNA modified tumor-derived exosomes as novel tools for maturation of dendritic cells. *J Cell Physiol* 2019; 234: 9417–9427.
2018/10/27
. DOI: 10.1002/jcp.27626.

52. Livak KJ and Schmittgen TD. Analysis of relative gene expression data using real-time quantitative PCR and the 2(-Delta Delta C(T)) Method. *Methods* 2001; 25: 402-408. 2002
/02/16
. DOI: 10.1006/meth.2001.1262.

53. Ji H, Greening DW, Barnes TW, et al. Proteome profiling of exosomes derived from human primary and metastatic colorectal cancer cells reveal differential expression of key metastatic factors and signal transduction components. *Proteomics* 2013; 13: 1672-1686. 2013
/04/16
. DOI: 10.1002/pmic.201200562.

54. Nie F, Cao J, Tong J, et al. Role of Raf-kinase inhibitor protein in colorectal cancer and its regulation by hydroxycamptothecine. *Journal of Biomedical Science* 2015; 22: 56. DOI: 10.1186/s12929-015-0162-y.

55. Leicht DT, Balan V, Kaplun A, et al. Raf kinases: function, regulation and role in human cancer. *Biochim Biophys Acta* 2007; 1773: 1196–1212.
2007/06/09
. DOI: 10.1016/j.bbamcr.2007.05.001.

56. Vafaei S, Saeednejad Zanjani L, Habibi Shams Z, et al. Low expression of Talin1 is associated with advanced pathological features in colorectal cancer patients. *Sci Rep* 2020; 10: 17786.
2020/10/22
. DOI: 10.1038/s41598-020-74810-6.

57. Fares J, Fares MY, Khachfe HH, et al. Molecular principles of metastasis: a hallmark of cancer revisited. *Signal Transduction and Targeted Therapy* 2020; 5: 28. DOI: 10.1038/s41392-020-0134-x.
58. Tickner JA, Urquhart AJ, Stephenson SA, et al. Functions and therapeutic roles of exosomes in cancer. *Front Oncol* 2014; 4: 127. 2014/06/07. DOI: 10.3389/fonc.2014.00127.
59. Vafaei S, Roudi R, Madjd Z, et al. Potential theranostics of circulating tumor cells and tumor-derived exosomes application in colorectal cancer. *Cancer Cell Int* 2020; 20: 288. 2020/07/14 . DOI: 10.1186/s12935-020-01389-3.
60. Papadaki MA, Stoupis G, Theodoropoulos PA, et al. Circulating Tumor Cells with Stemness and Epithelial-to-Mesenchymal Transition Features Are Chemoresistant and Predictive of Poor Outcome in Metastatic Breast Cancer. *Mol Cancer Ther* 2019; 18: 437–447. 2018/11/08 . DOI: 10.1158/1535-7163.MCT-18-0584.
61. Gkountela S and Aceto N. Stem-like features of cancer cells on their way to metastasis. *Biology Direct* 2016; 11: 33. DOI: 10.1186/s13062-016-0135-4.
62. Agnoletto C, Corrà F, Minotti L, et al. Heterogeneity in Circulating Tumor Cells: The Relevance of the Stem-Cell Subset. *Cancers (Basel)* 2019; 11: 483. DOI: 10.3390/cancers11040483.
63. Wang B, Wang Y, Yan Z, et al. Colorectal cancer cell-derived exosomes promote proliferation and decrease apoptosis by activating the ERK pathway. *Int J Clin Exp Pathol* 2019; 12: 2485–2495.
64. Conigliaro A and Cicchini C. Exosome-Mediated Signaling in Epithelial to Mesenchymal Transition and Tumor Progression. *J Clin Med* 2018; 8 2018/12/29. DOI: 10.3390/jcm8010026.
65. Mashouri L, Yousefi H, Aref AR, et al. Exosomes: composition, biogenesis, and mechanisms in cancer metastasis and drug resistance. *Mol Cancer* 2019; 18: 75. 2019/04/04. DOI: 10.1186/s12943-019-0991-5.
66. Lafitte M, Lecointre C and Roche S. Roles of exosomes in metastatic colorectal cancer. *Am J Physiol Cell Physiol* 2019; 317: C869-C880. 2019/07/11. DOI: 10.1152/ajpcell.00218.2019.
67. Steinbichler TB, Dudas J, Skvortsov S, et al. Therapy resistance mediated by exosomes. *Mol Cancer* 2019; 18: 58. 2019/03/31. DOI: 10.1186/s12943-019-0970-x.
68. Medeiros B and Allan AL. Molecular Mechanisms of Breast Cancer Metastasis to the Lung: Clinical and Experimental Perspectives. *Int J Mol Sci* 2019; 20 2019/05/11. DOI: 10.3390/ijms20092272.
69. Witwer KW, Buzas EI, Bemis LT, et al. Standardization of sample collection, isolation and analysis methods in extracellular vesicle research. *J Extracell Vesicles* 2013; 2 2013/09/07. DOI: 10.3402/jev.v2i0.20360.
70. Kong D, Li Y, Wang Z, et al. miR-200 regulates PDGF-D-mediated epithelial-mesenchymal transition, adhesion, and invasion of prostate cancer cells. *Stem Cells* 2009; 27: 1712-1721. 2009 /06/23 . DOI: 10.1002/stem.101.

71. Liu J, Liao S, Huang Y, et al. PDGF-D improves drug delivery and efficacy via vascular normalization, but promotes lymphatic metastasis by activating CXCR4 in breast cancer. *Clin Cancer Res* 2011; 17: 3638–3648.
2011/04/05
. DOI: 10.1158/1078-0432.CCR-10-2456.
72. Lahsnig C, Mikula M, Petz M, et al. ILEI requires oncogenic Ras for the epithelial to mesenchymal transition of hepatocytes and liver carcinoma progression. *Oncogene* 2009; 28: 638–650.
2008/11/19
. DOI: 10.1038/onc.2008.418.
73. Hosaka K, Yang Y, Seki T, et al. Tumour PDGF-BB expression levels determine dual effects of anti-PDGF drugs on vascular remodelling and metastasis. *Nat Commun* 2013; 4: 2129.
2013/07/09
. DOI: 10.1038/ncomms3129.
74. Verstraete M, Debucquoy A, Dekervel J, et al. Combining bevacizumab and chemoradiation in rectal cancer. Translational results of the AXEBeam trial. *Br J Cancer* 2015; 112: 1314–1325.
2015/04/14
. DOI: 10.1038/bjc.2015.93.
75. Zong S, Li W, Li H, et al. Identification of hypoxia-regulated angiogenic genes in colorectal cancer. *Biochem Biophys Res Commun* 2017; 493: 461–467. 2017/09/21. DOI: 10.1016/j.bbrc.2017.08.169.
76. Paulsson J, Ehnman M and Ostman A. PDGF receptors in tumor biology: prognostic and predictive potential. *Future Oncol* 2014; 10: 1695–1708.
2014/08/26
. DOI: 10.2217/fon.14.83.
77. Tian H, Yin L, Ding K, et al. Raf1 is a prognostic factor for progression in patients with nonsmall cell lung cancer after radiotherapy. *Oncol Rep* 2018; 39: 1966–1974.
2018/02/28
. DOI: 10.3892/or.2018.6277.
78. Jiang Q, Cheng L, Ma D, et al. FBXL19-AS1 exerts oncogenic function by sponging miR-431-5p to regulate RAF1 expression in lung cancer. *Biosci Rep* 2019; 39
2019/01/06
. DOI: 10.1042/BSR20181804.
79. Duan G and Walther D. The roles of post-translational modifications in the context of protein interaction networks. *PLoS Comput Biol* 2015; 11: e1004049-e1004049. DOI: 10.1371/journal.pcbi.1004049.
80. Edfors F, Danielsson F, Hallström BM, et al. Gene-specific correlation of RNA and protein levels in human cells and tissues. *Mol Syst Biol* 2016; 12: 883–883. DOI: 10.15252/msb.20167144.
81. Koussounadis A, Langdon SP, Um IH, et al. Relationship between differentially expressed mRNA and mRNA-protein correlations in a xenograft model system. *Scientific Reports* 2015; 5: 10775. DOI:

10.1038/srep10775.

82. Brion C, Lutz SM and Albert FW. Simultaneous quantification of mRNA and protein in single cells reveals post-transcriptional effects of genetic variation. *Elife* 2020; 9 2020/11/17. DOI: 10.7554/eLife.60645.

83. Greenbaum D, Colangelo C, Williams K, et al. Comparing protein abundance and mRNA expression levels on a genomic scale. *Genome Biol* 2003; 4: 117–117. 2003/08/29 . DOI: 10.1186/gb-2003-4-9-117.

Tables

Table 1 : Main characteristics of the ten proteins recovered in TDEs and CTCs

Gene name	Description	Metastasis-related	Stemness-related	Main Signaling Pathways
PDGFA	Platelet Derived Growth Factor Subunit A	yes	yes	Notch1/Twist1 pathway Wnt signaling related to EGFR and STAT3 constitutive signaling by aberrant PI3K in cancer cell proliferation and migration survival and chemotaxis
RNF11	Ring finger protein 11	unknown	unknown	related to NFkB and EGFR essential component of an ubiquitin-editing protein complex
TPTE	Transmembrane Phosphatase with Tensin Homology	yes	unknown	Pten-related tyrosine phosphatase signal transduction pathway of endocrine or spermatogenic functions of the testis
PPP3R1	Protein Phosphatase 3 Regulatory Subunit Bα	unknown	unknown	regulatory subunit of calcineurin calcium-dependent Calmodulin stimulated protein phosphatase
UBE2H	Ubiquitin Conjugating Enzyme E2H	yes	unknown	protein metabolism Class I MHC mediated antigen processing and presentation hypoxia-related gene
YWHAH	Tyrosine 3 Monooxygenase / Tryptophane 5 Mono-oxygenase, Activation Protein Eta	yes	unknown	binding and adaptor protein kinase activity telomerase activity
YWHAZ	Tyrosine 3 Monooxygenase / Tryptophane 5 Mono-oxygenase, Activation Protein Zeta	yes	yes	binding and adaptor protein phospholipase activity catalytic activity MAP kinase activity
NPTN	Neuroplastin	yes	unknown	DNA and protein binding kinase activity
LDLTAP1	Low Density Lipoprotein Receptor, Adaptor Protein 1	yes	unknown	protein and receptor binding catalytic activity
CAPZA2	Capping Actin Protein of Muscle Z-Line Subunit Alpha 2	yes	yes	protein and receptor binding ATP binding Actin binding telomerase activity

Table 2. Patients and tumor pathological characteristic of the study population		
Patients and tumor characteristics	**Exosome genes N (%)**	**Microvesicle genes N (%)**
Gender **Male** **Female** **(Male/Female)**	 12 (60.0) 8 (40.0) 1.5	 8 (40.0) 12 (60.0) 0.6
Median age, years (Range) **≤Median age** **>Median age**	**59 years (29-81)** 12 (60.0) 8 (40.0)	**59 years (31-81)** 12 (60.0) 8 (40.0)
Tumor grade **Low** **High**	 11 (55.0) 8 (45.0)	 16 (80.0) 4 (20.0)
Nodal stage **Yes** **No**	 6 (30.0) 14 (70.0)	 7 (35.0) 13 (65.0)
Primary tumor (PT) stage **pT1** **pT2** **pT3** **PT4**	 2 (10.0) 8 (40.0) 6 (30.0) 4 (20.0)	 0 (0.0) 12 (60.0) 8 (40.0) 0 (0.0)
Total (N)	20	20

Table 3. The association between tumor exosome genes mRNA expression and clinicopathological parameters of colorectal cancer (CRC) samples (*P value*; Pearson's $\chi 2$ test)

Patients and tumor characteristics	Total samples N (%)	*PDGFA* mRNA expression (Cut off = 5.95) N (%)		*P-value*	*RAF1* mRNA expression (Cut off = 1.5) N (%)		*P-value*
		Low (≤ 5.95)	High (>5.95)		Low (≤ 1.50)	High (> 1.50)	
CRC patients	20	10 (50.0)	10 (50.0)		10 (50.0)	10 (50.0)	
Gender							
Male	12 (60.0)	7 (35.0)	5 (25.0)		7 (35.0)	5 (25.0)	
Female	8 (40.0)	3 (15.0)	5 (25.0)	0.210	3 (15)	5 (25.0)	0.210
(Male/Female)	1.5	2.3	1		2.3	1	
Median age 59, years (29-81)							
≤Median age	12 (60.0)	6 (30.0)	6 (30.0)	1.000	8 (40.0)	2 (10.0)	***0.050***
>Median age	8 (40.0)	4 (20.0)	4 (20.0)		2 (10.0)	8 (40.0)	
Histological grade							
Low	11 (55.0)	6 (30.0)	5 (25.0)	0.264	6 (30.0)	5 (25.0)	0.507
High	8 (45.0)	4 (20.0)	4 (20.0)		4 (20.0)	4 (20.0)	
Nodal stage							
Yes	6 (60.0)	3 (15.0)	3 (15.0)	0.373	3 (15.0)	3 (15.0)	0.606
No	14 (40.0)	6 (30.0)	8 (40.0)		6 (30.0)	8 (40.0)	
Primary tumor (PT) stage							
pT1	2 (10.0)	1 (5.0)	1 (5.0)		1 (5.0)	1 (5.0)	
pT2	8 (40.0)	4 (20.0)	4 (20.0)	0.813	4 (20.0)	4 (20.0)	0.454
pT3	6 (30.0)	3 (15.0)	3 (15.0)		2 (10.0)	4 (20.0)	
PT4	4 (20.0)	2 (10.0)	2 (10.0)		3 (15.0)	1 (5.0)	

Table 4. The association between tumor microvesicle genes mRNA expression and clinicopathological parameters of colorectal cancer (CRC) samples (*P value*; Pearson's $\chi 2$ test)

Patients and tumor characteristics	Total samples N (%)	*PDGFA* mRNA expression (Cut off = 0.22) N (%)		*P-value*	*RAF1* mRNA expression (Cut off = 0.10) N (%)		*P-value*
		Low (≤ 0.22)	High (> 0.22)		Low (≤ 0.10)	High (> 0.10)	
CRC patients	20	14 (70.0)	6 (30.0)		14 (70.0)	6 (30.0)	
Gender							
Male	8 (40.0)	5 (25.0)	3 (15.0)		6 (30.0)	2 (10.0)	
Female	12 (60.0)	9 (45.0)	3 (15.0)	0.500	8 (40.0)	4 (20.0)	0.690
(Male/Female)	0.6	0.5	1		0.75	0.5	
Median age 59, years (31-81)							
≤Median age	12 (60.0)	10 (50.0)	5 (25.0)	1.000	10 (50.0)	1 (5.0)	1.000
>Median age	8 (40.0)	4 (20.0)	1 (5.0)		4 (20.0)	5 (25.0)	
Histological grade							
Low	16 (80.0)	11 (55.0)	5 (25.0)		11 (55.0)	5 (25.0)	
High	4 (20.0)	3 (15.0)	1 (5.0)	0.445	3 (15.0)	1 (5.0)	0.560
Nodal stage							
Yes	7 (35.0)	3 (15.0)	4 (20.0)		2 (10.0)	5 (25.0)	
No	13(65.0)	6 (30.0)	7 (35.0)	0.498	5 (15.0)	8 (45.0)	0.500
Primary tumor (PT) stage							
pT1	0 (0.0)	0 (0.0)	0 (0.0)		0 (0.0)	0 (0.0)	
pT2	12 (60)	8 (40.0)	4 (20.0)	0.610	8 (40.0)	4 (20.0)	0.698
pT3	8 (40)	6 (30.0)	2 (10.0)		6 (30.0)	2 (10.0)	
PT4	0 (0.0)	0 (0.0)	0 (0.0)		0 (0.0)	0 (0.0)	

Figures

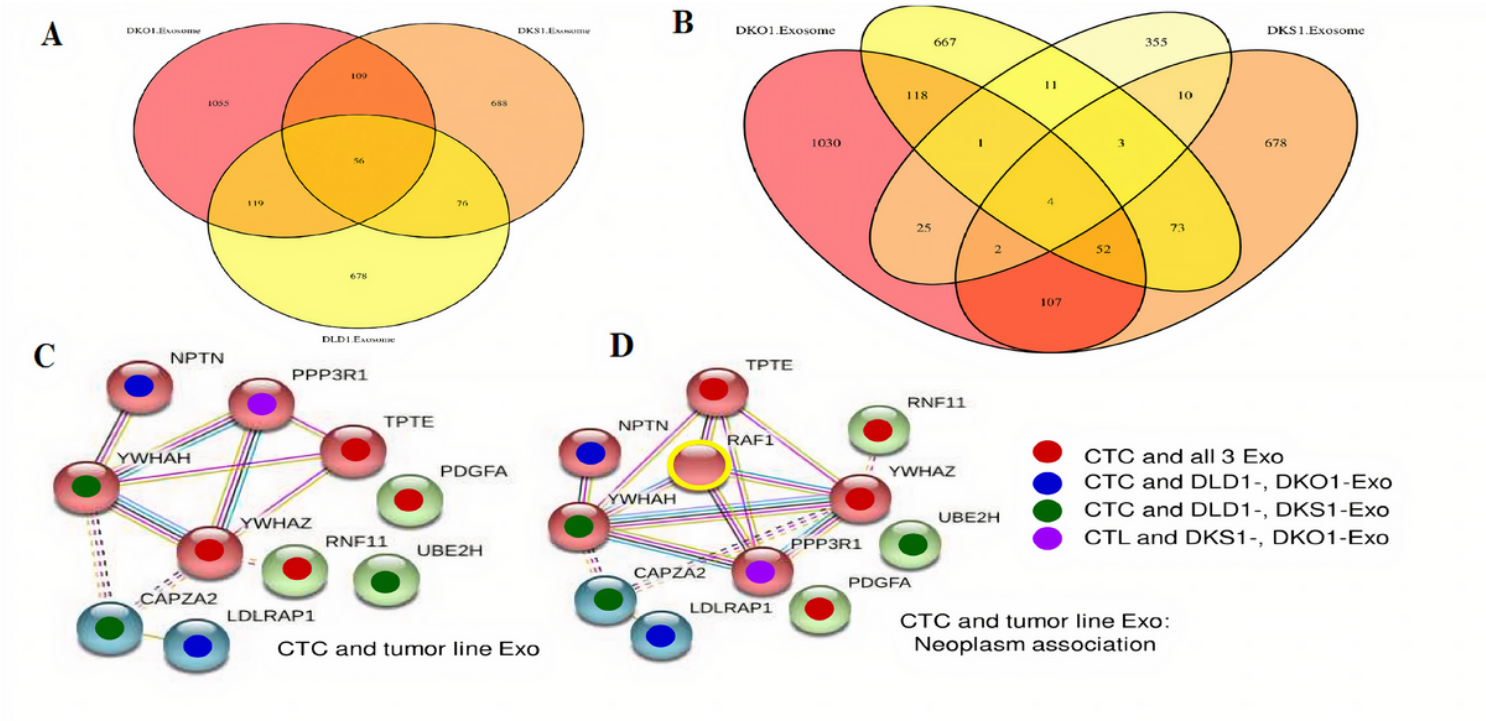

Figure 1

Distribution and protein-protein interaction network of genes in cell line-derived exosomes. (A) Distribution of genes in cell line-derived exosomes from three cell lines, where 56 markers were expresses in all three-cell line-derived exosomes (intersection). (B) Ten markers are expressed in at least two cell line-derived TDEs and CTCs. (C) Network and enrichment analysis for these 10 protein coding genes according to String functional protein clusters (kmeans). The strength of interaction is indicated by the thickness of the connecting lines. Recovery in CTC and all 3 or 2 Exo preparations is indicated by a colored dot. The network shows significantly more interactions than expected (p-value: 0.0156) (D) Network and enrichment analysis for these 11-tumor growth-associated protein coding genes according to String functional protein clusters (kmeans). The strength of interaction is indicated by the thickness of the connecting lines. Recovery in the 10 CTC and 3 or 2 Exo preparations is indicated by a colored dot. The central node is RAF1 (yellow circle). The network shows significantly more interactions than expected (p-value: 0.00639).

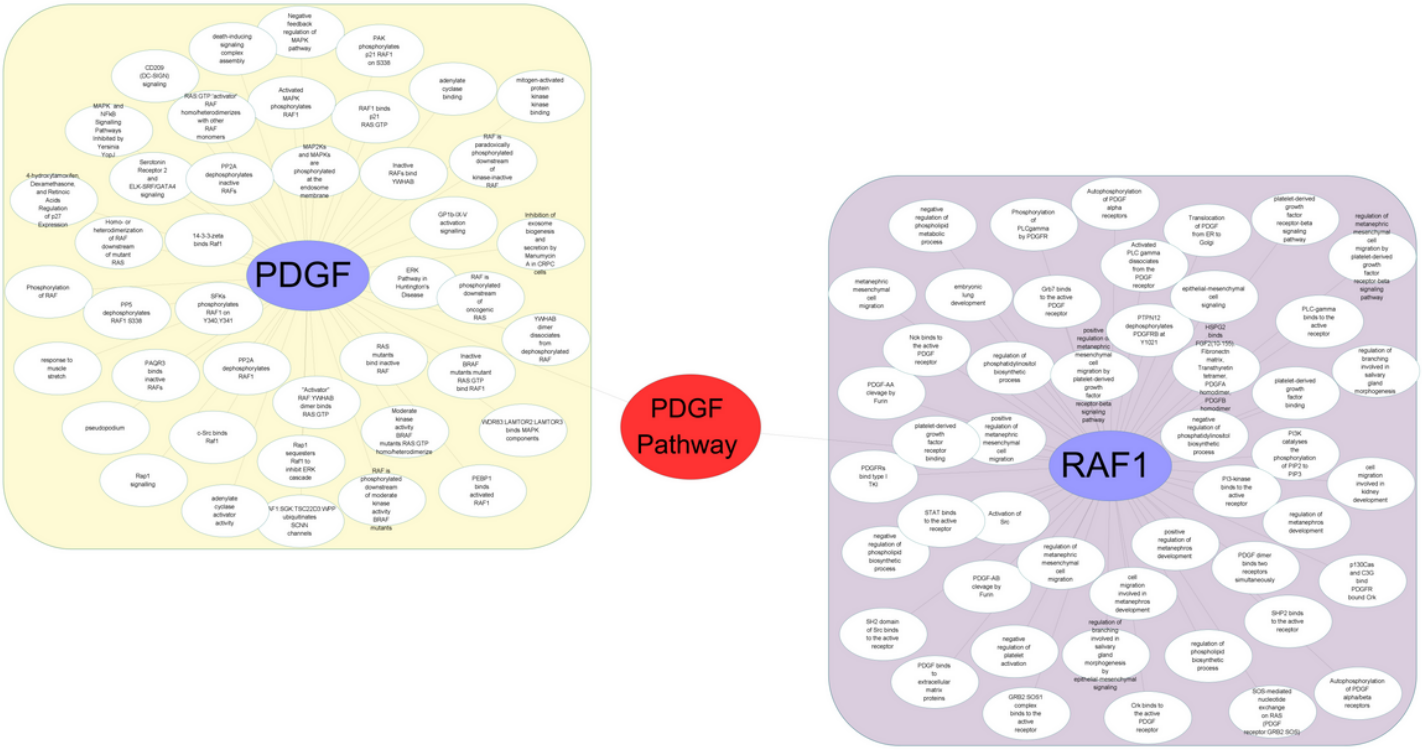

Figure 2

Pathway analysis using ClueGO plugin (Cytoscape) for PDGFA and RAF1. Pathway analysis indicated that PDGF Pathway is in common of both.

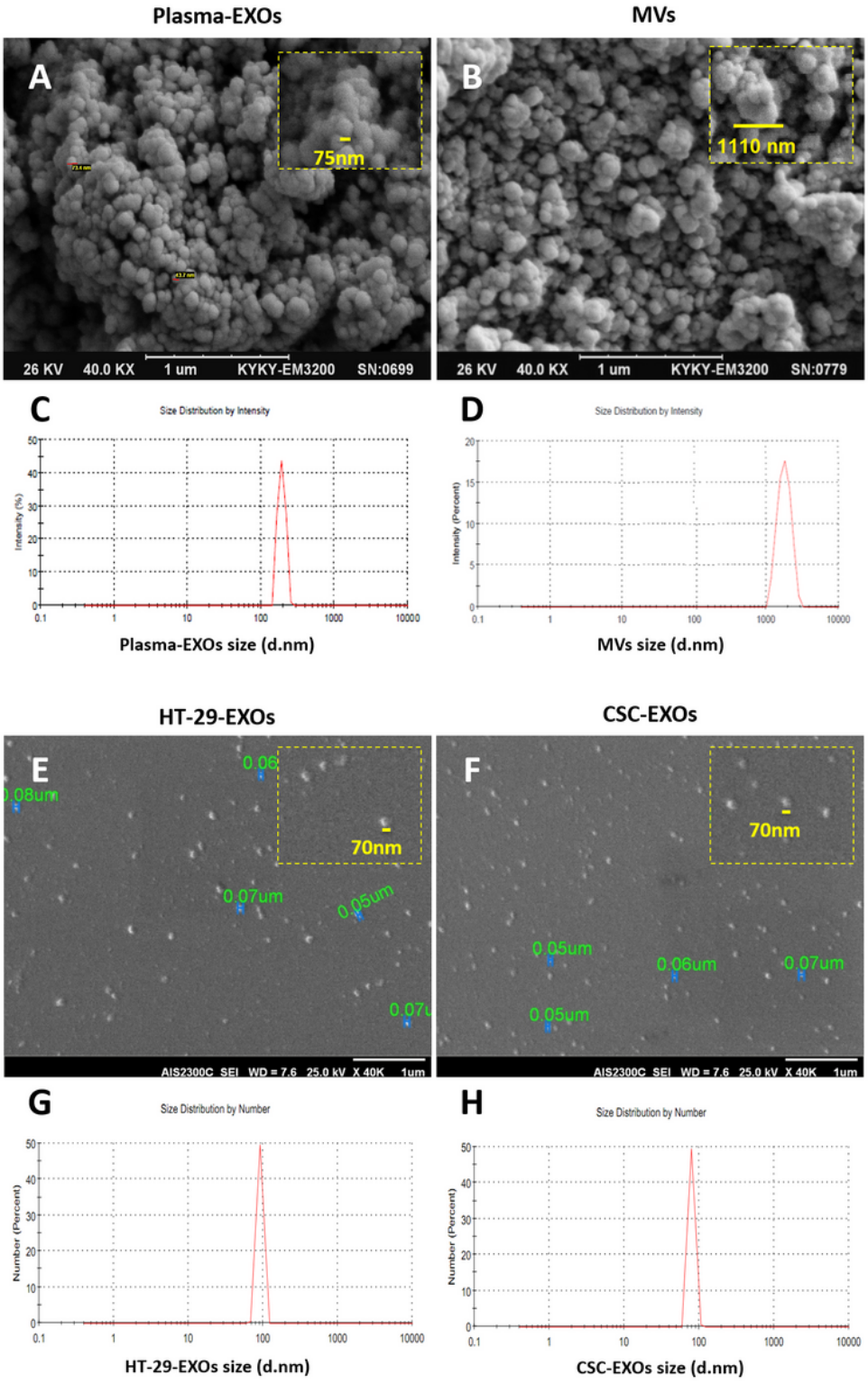

Figure 3

Exosome characterization. Representative SEM photograph of (A) plasma-EXOs and (B) MVs show homogenous round morphology. Exosome size distribution analysis of (C) plasma-EXOs and (D) MVs by DLS. Representative SEM photograph of (E) HT-29-EXOs and (F) CSC-EXOs. Exosome size distribution analysis of (G) HT-29-EXOs and (H) CSC-EXOs by DLS. Data are represented as mean ± SD (n = 3 each).

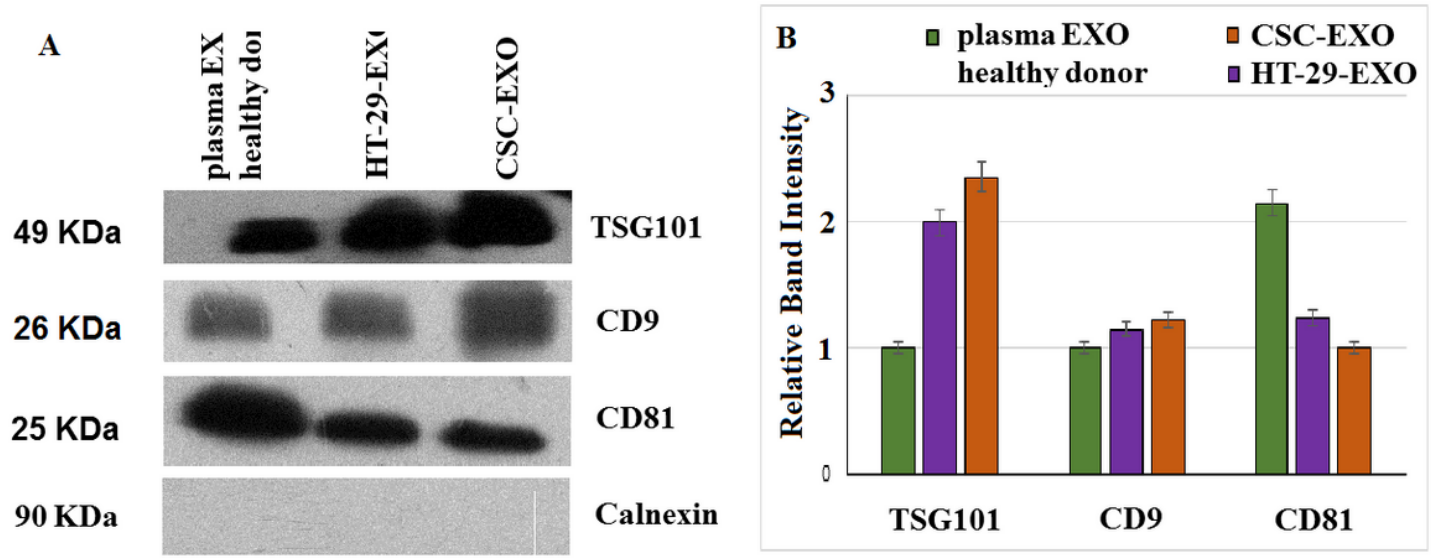

Figure 4

Western blot analysis of exosome surface marker expression. (A) Expression of TSG101, CD9, CD81 and, as a negative control calnexin, were evaluated by WB in plasma EXOs, CSC-EXOs, and HT-29-EXOs to confirm the exosomal characteristic of isolated exosomes. (B) The relative expression levels of exosomal markers of plasma EXOs, CSC-EXOs, and HT-29- EXOs. Data are represented as mean ± SD (n = 3).

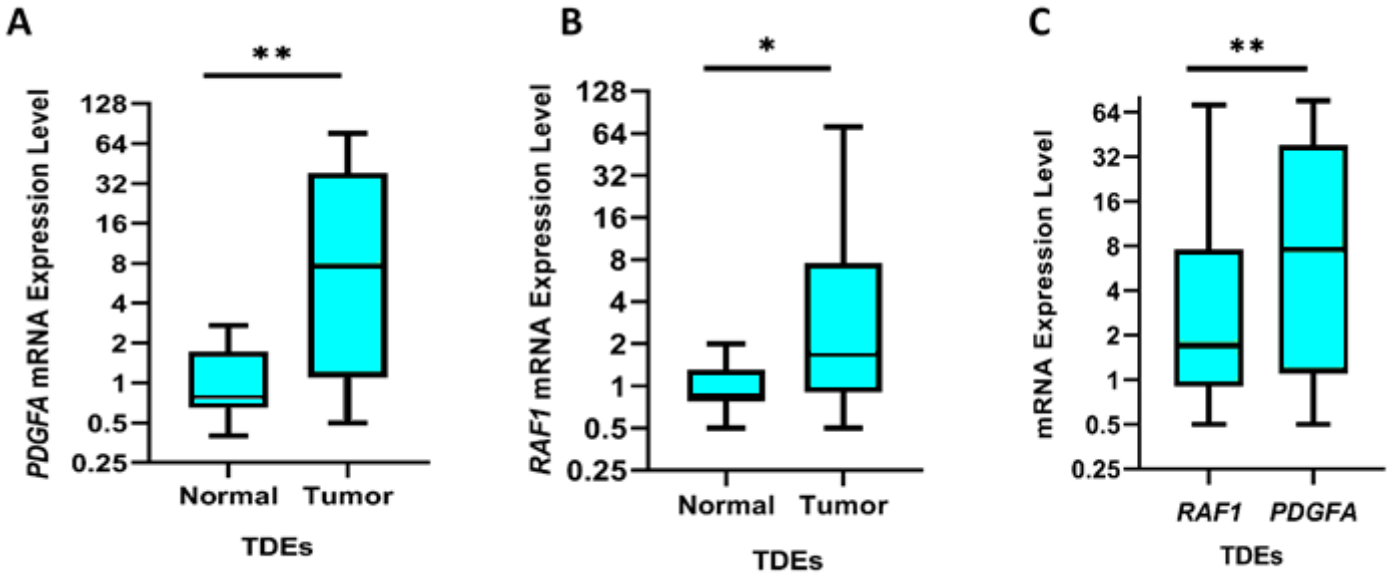

Figure 5

Real-time PCR analysis of PDGFA and RAF1 expression levels in TDEs. TDEs from CRC patients revealed a statistically significant differences between (A) median mRNA expression levels of PDGFA (P=0.0086) and (B) RAF1 (P=0.048) compared to healthy control samples. (C) A statically significant positive correlation was observed between PDGFA and RAF1 mRNA expression patterns in TDEs (P=0.0084). Data are represented as mean ± SD (n = 3). *P < 0.05 and **P < 0.01.

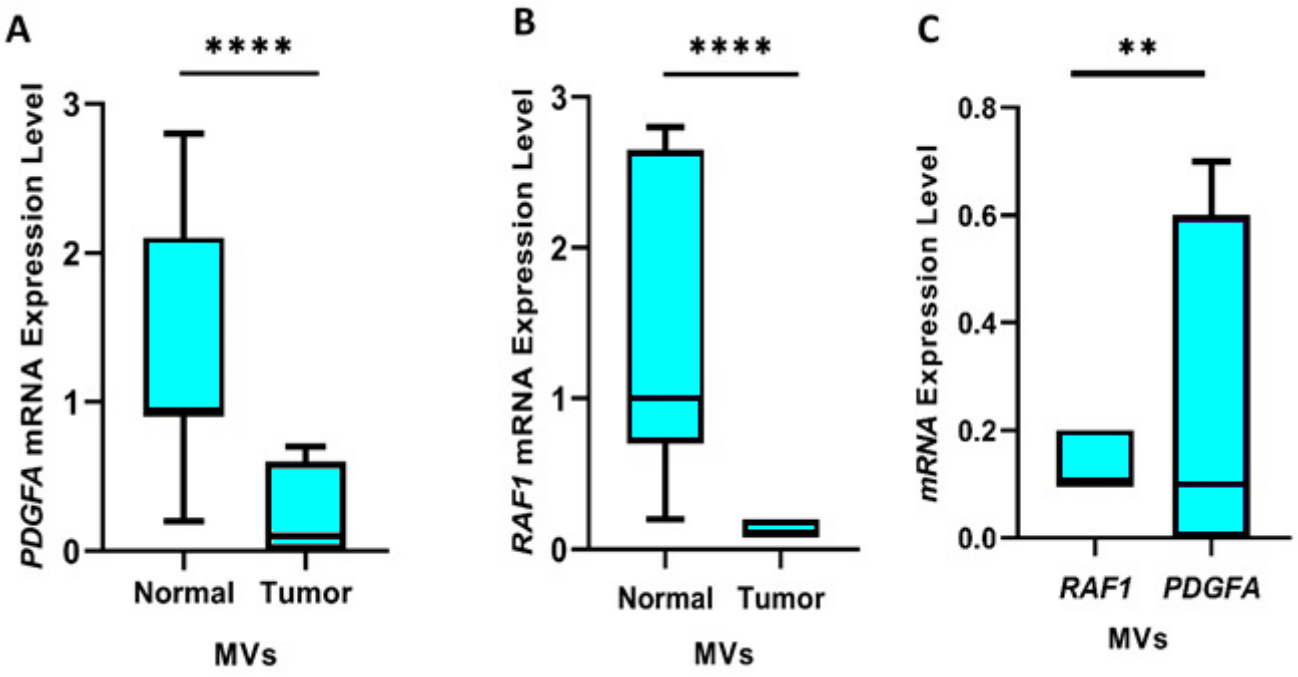

Figure 6

Real-time PCR analysis of PDGFA and RAF1 expression levels in MVs. MVs from CRC patients showed a statistically significant decrease in (A) median mRNA expression levels of PDGFA (P=0.0001) and (B) RAF1 (P=0.0001) compared to healthy control samples (C) A statically significant positive correlation was found between mRNA PDGFA and RAF1expression patterns in MVs (P=0.0084). Data are represented as mean ± SD (n = 3 each). **P < 0.01 and ****P < 0.0001.

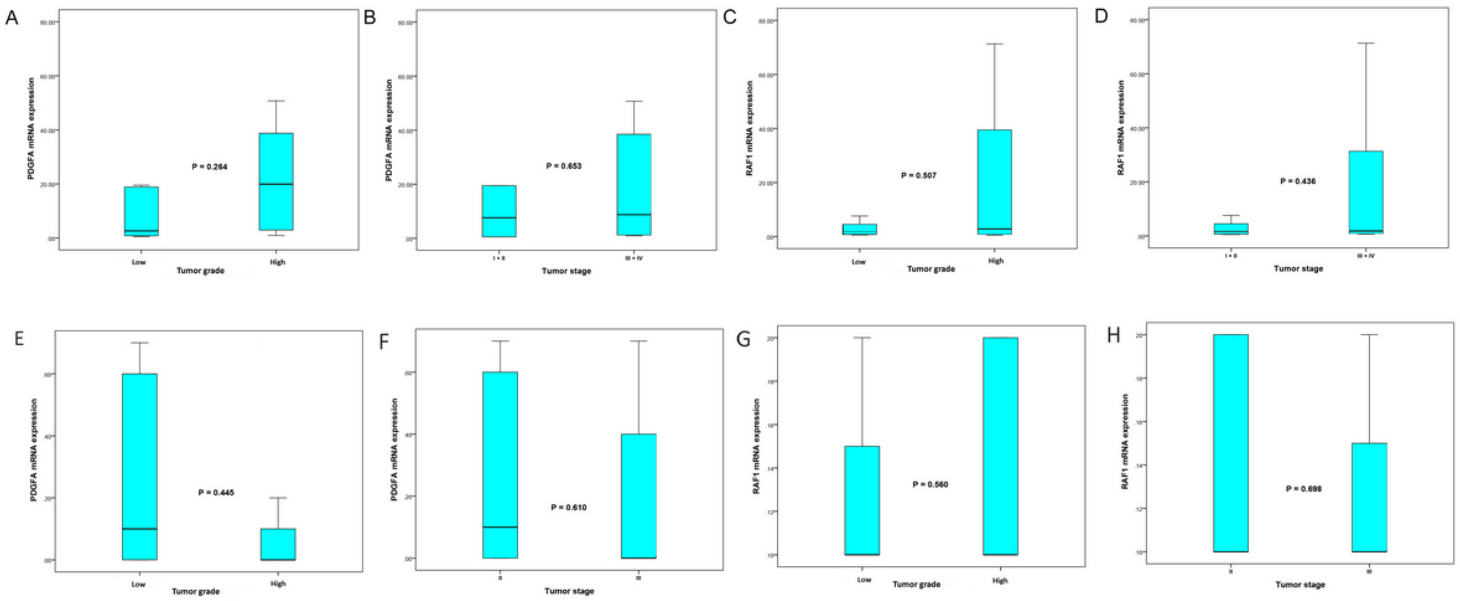

Figure 7

Box plot analysis of expression levels of tumor exosomes and tumor microvesicles in tumor grade low versus high and tumor stage I+II versus III+IV of colorectal cancer (CRC) patients using Mann–Whitney U test. (A), (B) The results showed that there are no statistically significant associations for median expression levels of PDGFA mRNA between tumor differentiation (low) versus (high) and tumor stage (I+II) versus (III+IV) (P = 0.264, P = 0.653, respectively), and also (C) (D) median expression levels of RAF1 mRNA between tumor differentiation (low) versus (high) and tumor stage (I+II) versus (III+IV) (P = 0.507, P = 0.436, respectively) in CRC patients. (E), (F) The results revealed that there are no statistically significant associations for median expression levels of PDGFA mRNA between tumor differentiation (low) versus (high) and tumor stage II versus III (P = 0.445, P = 0.610, respectively), and also (G), (H) median expression levels of RAF1 mRNA between tumor differentiation (low) versus (high) and tumor stage II versus III (P = 0.560, P = 0.698, respectively) in CRC cases. Based on the standard definitions, each box-plot shows the median (bold line) and interquartile lines (box). Data are represented as mean ± SD (n = 3). Though no significant differences in the median level of PDGFA and RAF1 mRNA expression in tumor exosomes of different grades or stages were seen, these results should be considered with caution taking into account the small numbers of samples.

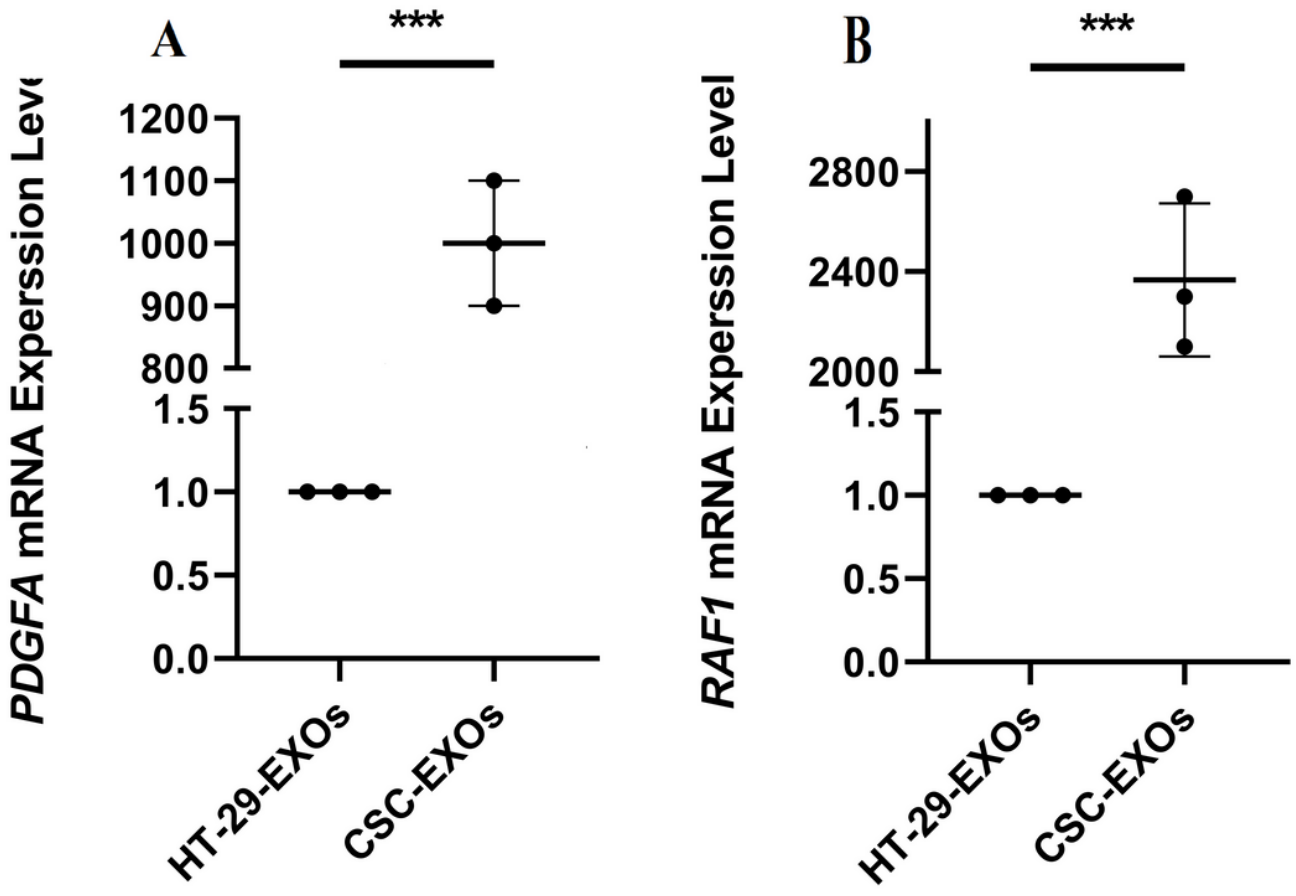

Figure 8

Real-time PCR analysis of PDGFA and RAF1 expression levels in CSC-EXOs compared to HT-29-EXOs. CSC-EXOs showed significantly increased expression of (A) PDGFA (P=0.0004) and (B) RAF1 (P=0.0004)

compared to HT-29-EXOs. Data are represented as mean ± SD (n = 3). ***P < 0.001.

Supplementary Files

This is a list of supplementary files associated with this preprint. Click to download.

- supplementarytable1.xlsx
- supplementarytable2.xlsx
- supplementarytable3.xlsx
- supplementarytable4.xlsx
- SupplementaryTable5.xlsx
- supplementaryfigure1.tif